



L OVELY
P ROFESSIONAL
U NIVERSITY

Report

on

Topic:- Satellite farming using remote sensing images/ drone images

Submitted by:
Ashish Kumar

Registration No:11717701

Section:-KM030

ROLL NO:-26

Programme Name:

BTECH.COMPUTER SCIENCE AND ENGINEERING

Under the Guidance of

Mr Sanjay Kumar Singh

Assistant Professor

The discipline of CSE/IT
School of Computer Science & Engineering
Lovely Professional University, Phagwara

Satellite farming using remote sensing images/ drone images

By Ashish Kumar and Hariom Jha

Abstract

For better agricultural productivity and food management, there is an urgent need for precision agriculture monitoring at larger scales. In recent years, drones have been employed for precision agriculture monitoring at smaller scales, and for the past few decades, satellite data are being used for land cover classification and agriculture monitoring at larger scales. The monitoring of agriculture precisely over a large scale is a challenging task. In this paper, an approach has been proposed for precision agriculture monitoring, i.e., the classification of sparse and dense fields, which is carried out using freely available satellite data (Landsat 8) along with drone data. Repeated usage of drone has to be minimized and hence an adaptive classification approach is developed, which works with image statistics of the selected region. The proposed approach is successfully tested and validated on different spatial and temporal Landsat 8 data.

Index Terms—Adaptive thresholding, drone, Landsat 8, precision agriculture monitoring, satellite images.

INTRODUCTION

AGRICULTURE has a prime role in the Indian economy, as it shares about 17% of GDP and employs about 50% of the workforce. For better agricultural production and food management, providing key ideas through precision agriculture monitoring is important. Precision agriculture is a crop management concept that is field-specific and is more helpful for better productivity. Precision

agriculture makes use of real-time information from sensors and geospatial techniques (remote sensing, geographic information system) and helps in making smarter decisions for better productivity. The use of wireless sensor networks for precision agriculture is widely discussed in and, which employs wireless sensors directly in the field to collect and transmit information to a data processing centre through the network. Usage of drones or unmanned aerial vehicle for precision agriculture is the latest trend. With the easy availability of commercial drones at affordable costs, farmers can use them for monitoring their farms. However, in countries like India, where all cannot afford such a monitoring system, people are still dependent on the physical inspection of the crops. Thus, a solution at the global level is required and satellite images are widely used for the same. The fusion of satellite image with drone image for precision agriculture monitoring is an important task to be explored.

Land-cover classification into classes like water, vegetation, bare land, urban, etc., is researched for many years and several supervised and unsupervised classification approaches are available, such as decision tree, neural network, object-based image analysis, support vector machine, and time-series analysis. Crop-type classification with the help of spectral signatures from hyperspectral and temporal signatures from time-series multispectral images has also been carried out by many researchers. Satellite images are also downscaled to provide better

spatial resolution and some of the commonly used downscaling techniques are probabilistic model-based, sensor-based, learning-based, scaling laws, frequency representation, and panchromatic sharpening.

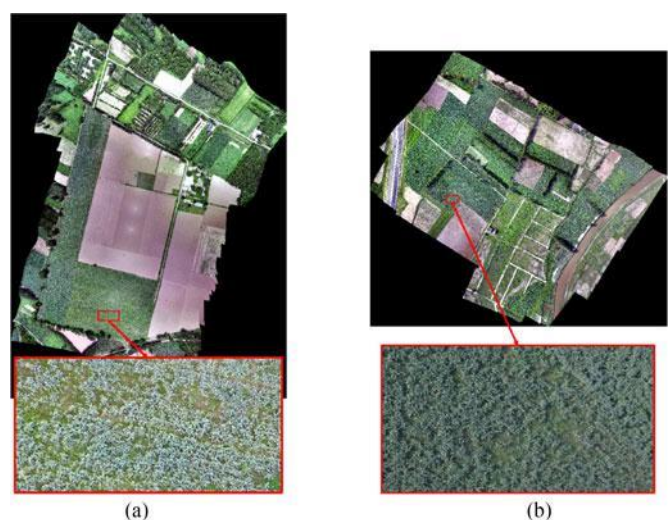
Satellite images are used for applications such as the identification of sparse shrublands and sparse grasslands for desertification monitoring with the accuracy of 79% and 66%, respectively; quantifying sparse vegetation cover with mixture modelling using aircraft-based Probe-1 hyperspectral imagery, etc. However, within class classification such as the segregation of vegetation regions into sparse and dense regions in a large field using satellite imagery, a part of precision agriculture monitoring has not been explored yet. There is a need for precision agriculture monitoring at large scale and synergetic use of satellite data along with drone imagery might help solve such problems, as drone images can provide precise ground truth information. Researchers have used only drone images for precision agriculture monitoring applications like crop biomass monitoring, water stress in crops, detecting small weed patches, for mapping vineyard vigour, and examining the results of various nitrogen treatments on crops. In all these approaches, we have to fly a drone every time to obtain the results. Therefore, the emphasis was on carrying out the fusion of drone and satellite data only once, and then use satellite data alone for other locations/data without the requirement of drone images. The main aim of this paper is to develop such a technique by which the repetitive usage of the drone can be minimized without affecting the results of

precision agriculture monitoring. For this purpose, we have developed an adaptive thresholding approach with the help of the fusion of satellite (Landsat 8) and drone data. After the development of the methodology, we can directly use the

satellite data without the requirement of drone data for a similar type of field.

STUDY AREA AND DATA USED

Agriculture fields around Roorkee in Haridwar district, Uttarakhand, India are chosen as a study area for this study. Sugarcane is one of the most prominent crops cultivated in the district of Haridwar, and more than 50% of the cultivable area in this district is used for sugarcane cultivation. Data are available in the form of tiles and the tile selected for this study covers the Haridwar district of Uttarakhand, India, along with some parts of neighbouring districts. Fig. 1(a) shows a false-colour composite (FCC) image of Landsat 8 data of Roorkee Tehsil with near-infrared (NIR), red, and green bands, and the two study areas are marked as Loc1 and Loc2. Details of Landsat 8 tiles used are listed in Table I. Landsat data down-loaded are stored as quantized and calibrated digital numbers.



MODEL DEVELOPMENT AND IMPLEMENTATION

This approach aims to distinguish sparse and dense vegetation within a large agriculture field. For developing this approach, only sugarcane fields are considered, and various steps used were critically analyzed and performed, which are described in the following subsections.

A. Cloud Masking

Optical data are generally affected by the cloud. For applications such as agriculture monitoring, which is to be performed in real-time, only the images available could be used. But using cloud-affected data might lead to misleading information due to altered reflectance values. So, there is a need to mask cloud-affected data before proceeding for further analysis. Landsat 8 data are provided with a quality assessment band, which consist of 16 flag bits. High state i.e., '1' in the 14th and 15th flag bits indicates the presence of a cloud in the selected pixel, and the mask is thus created using this information. The obtained mask is verified with the mask obtained using cloud detection technique described in. The percentage of cloud-affected area for Roorkee Tehsil in data L8A and L8B was found out to be 17.6% and 7.8%, respectively. It is observed that a subset of L8A data for Loc1 had cloud-affected pixels in it. Since L8B data are not affected by cloud and Loc1 sugarcane field having a similar proportion of sparse and dense areas, drone data Loc1B and Landsat data L8B are used for initial analysis.

B. Drone Image Segmentation and Gridding

Subset image from drone image is cropped with the help of upper left and lower right coordinates obtained from Landsat data subset. The spatial resolution of drone data is 6 cm and that of Landsat data is 30 m. Segments of 30 m × 30 m are made out of drone image with the same area corresponding to each pixel of Landsat data subset. This is achieved by using the corresponding coordinates of each Landsat pixel as a centre co-ordinate of each drone segment and segmenting it by selecting the required number of pixels around it. Similarly, the whole drone image subset is segmented into 30 m × 30 m segments corresponding to the Landsat data. Grids of 5 × 5 are made over each of the drone image segment, which corresponds to 6 m × 6 m in-ground resolution for each grid. Fig. 3(a) and (b) shows gridded segments of dense and sparse locations, respectively, of the same field.

C. Vegetation Extraction

In this paper, sugarcane fields are the main area of interest. During the field survey, areas of sugarcane field are marked and verified with drone images. The segments obtained by the procedure discussed in Section III-B are used for the selection of pixels in the Landsat image. Vegetation (sugarcane) mask is thus obtained by selecting all pixels in the Landsat image that corresponds to sugarcane, as shown in Fig. 4(a). Using the obtained mask, the spectral information of all the sugarcane pixels in the Landsat data is extracted for further analysis.

D. Ground Truth Data Collection

With the help of the mask obtained, the percentage of dense vegetation area for sugarcane segments has to be computed. Regions with sparse sugarcane plantations have been marked based on ground survey data and careful inspection of a drone image. Using the grids shown in Fig. 3, each grid is marked as sparse or dense regions. There are a total of 25 grids in each segment and the percentage of dense area is then computed using the following equation:

$$\% \text{ Dense area} = \frac{\text{Total no. of dense grids}}{25} \times 100 \quad (2)$$

Segments with percentage dense area below 70% are assigned as sparse segments [28]. A total of 71 segments are present, of which approximately 47 segments are sparse and the remaining 24 are dense segments. Fifteen segments of most sparse and most dense segments are chosen based on their dense area percentage and used as ground truth data for further analysis.

E. Band Selection for Sparse and Dense Classification

Once the sparse and dense segments are chosen from the drone image, its corresponding spectral reflectance values for bands green, red, NIR, SWIR1, SWIR2, and NDVI (normalized difference vegetation index) are extracted from the Landsat data. Mean and standard deviation for both the classes are computed for the selected six bands. Separability index (SI), a measure used to identify the class separability, is used to

identify the band that is best suitable for segregation of sparse and dense classes and is computed using the following equation:

$$SI_{i,j} = \frac{|\mu_i - \mu_j|}{\sigma_i + \sigma_j}$$

where μ and σ are the statistical mean and standard deviation of classes i and j , respectively.

Adaptive Thresholding

Once the band for classification is selected, there is a need to classify the data into two classes, sparse and dense vegetation by thresholding. Otsu thresholding is applied for obtaining the threshold value th_{in} . The main drawback of this technique is that ground truth data, which is obtained from the drone image, are mandatory information for each area of interest that is to be classified. It is not possible to fly the drone each time over the area of interest, and hence an adaptive technique is required, which can handle the change in the spatial and temporal variation of the image. To overcome this problem, an adaptive thresholding method is used. To identify the sparse region in the vegetation for precision monitoring of a particular field, we have applied gridding as discussed in Section III-B and the sparse region is computed using Then, we have assessed the overall accuracy (OA) based on how many sparse grids over the sparse region are identified by the proposed algorithm. To obtain the sparse segment in the Landsat image, we have proposed an adaptive thresholding technique that is discussed in the following subsection.

1) *Proposed Adaptive Thresholding Technique:*

The threshold (th) is calculated as follows: where μ and σ are the mean and standard deviation of all the vegetation pixels in the image, respectively, and n (usually varied from -1 to 1 in steps of 0.1) an unknown term whose value is selected in such a way that the two classes are classified with maximum accuracy. Two performance metrics, such as overall accuracy (OA) and false alarm rate (FAR), are used to determine the correctness of the value of n obtained as given in the following equations

$$OA = \frac{\text{No. of correctly detected sparse pixels}}{\text{Total no. of sparse pixels}}$$

$$FAR = \frac{\text{No. of dense pixels classified as sparse}}{\text{Total no. of pixels} - \text{Total no. of sparse pixels}}$$

RESULTS AND DISCUSSION

A. *Implementation Results*

Landsat data are preprocessed and cloud-affected pixels are masked using the generated cloud mask. With the help of a drone image, a subset of Landsat data is created. The vegetation mask is then created, as shown in Fig. 4(a), using drone image and markings from the ground survey. Drone image subset is segmented into segments of a size corresponding to the spatial resolution of Landsat data and gridded with 5×5 grids in each segment. Percentage of the sparse and dense area in each segment of the image is computed by

identifying grids in the segment as a sparse or dense grid, using the knowledge from the ground survey and close inspection of a drone image. This information serves as ground truth, by which band for segregation of sparse and dense class is selected with the help of SI. Theoretically and by the use of SI, it is noted that SWIR1 is best suited for this classification. Once the band is selected, the threshold is selected using an adaptive thresholding technique based on the image statistics and user-defined boundary conditions. The image is classified into sparse and dense areas.

The confusion matrix suggests that the proposed technique can produce highly consistent classification results relative to the reference data, as producer accuracy of sparse and dense vegetation classes obtained are 90% and 83.87%, respectively. Producer accuracy depends upon the error of omission which should be as less as possible for better accuracy. On the other hand, user accuracy corresponds to the error of commission which should also be as less as possible as in the case of producer accuracy. Commission errors obtained. for both, the. Therefore, user accuracy obtained is satisfactory, i.e., 87.80% and 86.66% for sparse and dense vegetation classes, respectively. User accuracy is a good parameter for accuracy assessment of a classifier as it provides the accuracy of the technique developed from the perspective of the user of the classified map. Moreover, OA and FAR are also computed and found out to be 87.32% and 16.13%, respectively, since a total of 62 pixels for both classes are classified correctly out of 71 pixels and only 5 pixels out of 31 pixels

of dense vegetation class are being misclassified into sparse vegetation class.

B. Validation

The developed approach is then validated by applying it over a different image that is different by location and date of acquisition. Drone image Loc2A and Landsat image L8A are selected for this purpose, and a subset of L8A is taken for the same area as in Loc2A. The vegetation mask is obtained as discussed in Section III-C and is shown in Fig. 7(a). Reflectance values of the SWIR1 band are extracted for the pixels in the mask. Mean and standard deviation of the selected pixels are calculated and used in the developed adaptive thresholding approach to determine the optimized value of n . For this image, the lower bound for OA (Lisboa) is kept the same as in the previous image, but the upper bound for FAR (ub_{FAR}) is changed to 10% for convergence. Then, the image is classified using the threshold value obtained from the optimized n value

To determine the accuracy of the classified image, the drone image is segmented into the size of an individual pixel of the Landsat image and 5×5 grids are made. Each grid is identified for the sparse or dense grid and percentage of the sparse and dense area within the segment is computed.

V. CONCLUSION

In this paper, an approach to segregate sparse and dense areas within a selected sugarcane field is developed and implemented uses the fusion of drone and satellite images for developing an adaptive approach by which the repetitive usage of the drone could be minimized. The

approach is made adaptive by using image statistics and finding threshold using a multiobjective optimization technique to maximize the OA and minimize the FAR. The results show that the approach has proven to be satisfactory for the classification between sparse and dense classes with an accuracy of about 87% and 73% for testing and validation data, respectively. To develop this algorithm the drone data are segmented into the spatial dimension of the satellite image and ground truth data are obtained by ground survey and careful inspection of gridded drone data. The proposed approach has the potential to be extended to different sensor data, as the developed approach is based on the image statistics. In the era of the digital world, this approach may be quite useful and applicable to users, such as government agricultural agencies, policymakers, farmers, and also insurance agencies for Fasal Bima Yojana, India

REFERENCES

- [1] D. J. Mulla, "Twenty five years of remote sensing in precision agriculture: Key advances and remaining knowledge gaps," *Biosyst. Eng.*, vol. 114, pp. 358–371, Apr. 2013.
- [2] A. McBratney, B. Whelan, T. Ancel, and J. Bouma, "Future directions of precision agriculture," *Precis. Agric.*, vol. 6, pp. 7–23, Feb. 2005.
- [3] A. Baggio, "Wireless sensor networks in precision agriculture," in *Proc. ACM Workshop Real-World Wireless Sensor Netw.*, Stockholm, Sweden, 2005, pp. 1567–1576.
- [4] N. Wang, N. Zhang, and M. Wang, "Wireless sensors in agriculture and food industry—Recent development

- and future perspective,” *Comput. Electron. Agric.*, vol. 50, pp. 1–14, Jan. 2006.
- [5] C. Zhang and J. M. Kovacs, “The application of small unmanned aerial systems for precision agriculture: A review,” *Precis. Agric.*, vol. 13, pp. 693–712, Jul. 2012.
- [6] D. Lu and Q. Weng, “A survey of image classification methods and techniques for improving classification performance,” *Int. J. Remote Sens.*, vol. 28, pp. 823–870, Mar. 2007.
- [7] P. Mishra and D. Singh, “A statistical-measure-based adaptive land cover classification algorithm by efficient utilization of polarimetric SAR observables,” *IEEE Trans. Geosci. Remote Sens.*, vol. 52, no. 5, pp. 2889–2900, May 2014.
- [8] T. Blaschke, “Object-based image analysis for remote sensing,” *ISPRS J. Photogramm. Remote Sens.*, vol. 65, pp. 2–16, Jan. 2010.
- [9] Y. Shao, R. S. Lunetta, B. Wheeler, J. S. liams, and J. B. Campbell, “An evaluation of time-series smoothing algorithms for land-cover classifications using MODIS-NDVI multi-temporal data,” *Remote Sens. Environ.*, vol. 174, pp. 258–265, Mar. 2016.
- [10] N. R. Rao, P. K. Garg, and S. K. Ghosh, “Development of a crops spectral library and classification of crops at cultivar level using hyperspectral data,” *Precis. Agric.*, vol. 8, pp. 173–185, Oct. 2007.
- [11] M. Govender, K. Chetty, and H. Bulcock, “A review of hyperspectral remote sensing and its application in vegetation and water resource studies,” *Water SA*, vol. 33, pp. 145–151, Jan. 2007.
- [12] Y. Zhou *et al.*, “Mapping paddy rice planting area in rice-wetland coexistent areas through analysis of Landsat 8 OLI and MODIS images,” *Int. J. Appl. Earth Obs. Geoinf.*, vol. 46, pp. 1–12, Apr. 2016.
- [13] R. Molina, M. Vega, J. Mateos, and A. K. Katsaggelos, “Variational posterior distribution approximation in Bayesian super-resolution reconstruction of multispectral images,” *Appl. Comput. Harmon. Anal.*, vol. 24, no. 2, pp. 251–267, 2008.
- [14] S. Nakazawa and A. Iwasaki, “Super-resolution imaging using remote sensing platform,” in *Proc. IEEE Int. Geosc. Remote Sens. Symp.*, 2014, pp. 1987–1990.
- [15] S. Baker and T. Kanade, “Limits on super-resolution and how to break them,” *IEEE Trans. Pattern Anal. Mach. Intell.*, vol. 24, no. 9, pp. 1167–1183, Sep. 2002.

Python implementation screenshot(Finding if the land is Grassland or Barrenland or other with the help of Satellite using remote sensing images/ drone images)

```
machine learning project(Satellite farming using remote sensing images/ drone images) ☆
File Edit View Insert Runtime Tools Help All changes saved
+ Code + Text
RAM
Disk

[ ] from google.colab import drive
drive.mount('/content/drive', force_remount=True)
# access key: 4/ygG3q1Uk4qD_tdrGmQ2pQhrZztW8B0vc1MuI71UfRqxC-sRnBtRKE

Mounted at /content/drive

[ ] import numpy as np # linear algebra
import pandas as pd # data processing, CSV file I/O (e.g. pd.read_csv)
import matplotlib.pyplot as plt # visualize satellite images
from skimage.io import imshow # visualize satellite images

from keras.layers import Dense, Conv2D, MaxPooling2D, Flatten, Dropout # components of network
from keras.models import Sequential # type of model

Using TensorFlow backend.

[ ] x_train_set_fpath = '/content/drive/My Drive/X_test_sat4.csv'
y_train_set_fpath = '/content/drive/My Drive/y_test_sat4.csv'
print('Loading Training Data')
X_train = pd.read_csv(x_train_set_fpath)
print('Loaded 28 x 28 x 4 images')

Y_train = pd.read_csv(y_train_set_fpath)
print('Loaded labels')

Loading Training Data
Loaded 28 x 28 x 4 images
Loaded labels

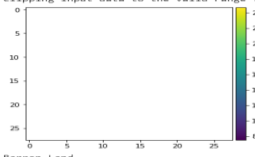
[ ] X_train = X_train.to_numpy()
Y_train = Y_train.to_numpy()
print('We have',X_train.shape[0],'examples and each example is a list of',X_train.shape[1],'numbers with',Y_train.shape[1],'possible classifications.')

We have 99999 examples and each example is a list of 3136 numbers with 4 possible classifications.
```

```
machine learning project(Satellite farming using remote sensing images/ drone images) ☆
File Edit View Insert Runtime Tools Help All changes saved
Code + Text
RAM
Disk

else:
    print('Other')

/usr/local/lib/python3.6/dist-packages/skimage/io/_plugins/matplotlib_plugin.py:150: UserWarning: Float image out of standard range; displaying image with stretched contrast.
  lo, hi, cmap = _get_display_range(image)
Clipping input data to the valid range for imshow with RGB data ([0..1] for floats or [0..255] for integers).



[ ] model = Sequential([
    Dense(4, input_shape=(3136,), activation='softmax')
])

[ ] X_train = X_train/255

[ ] model.compile(optimizer='adam', loss='categorical_crossentropy', metrics=['accuracy'])
model.summary()
model.fit(X_train,Y_train,batch_size=32, epochs=5, verbose=1, validation_split=0.01)

Model: "sequential_1"
Layer (type) Output Shape Range #
```

```
machine learning project(Satellite farming using remote sensing images/ drone images) ☆
File Edit View Insert Runtime Tools Help All changes saved
+ Code + Text
RAM
Disk

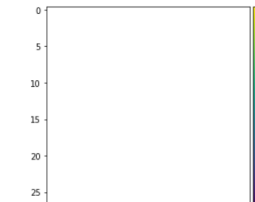
[ ] #First we have to reshape each of them from a list of numbers to a 28*28*4 image.
X_train_img = X_train.reshape([99999,28,28,4]).astype(float)
print(X_train_img.shape)

(99999, 28, 28, 4)

#Let's take a look at one image. Keep in mind the channels are R,G,B, and I(Infrared)
ix = 5 #Type a number between 0 and 99,999 inclusive
imshow(np.squeeze(X_train_img[ix,:,:,:]).astype(float)) #Only seeing the RGB channels
plt.show()

#Tells what the image is
if Y_train[ix,0] == 1:
    print('Barren Land')
elif Y_train[ix,1] == 1:
    print('Trees')
elif Y_train[ix,2] == 1:
    print('Grassland')
else:
    print('Other')

/usr/local/lib/python3.6/dist-packages/skimage/io/_plugins/matplotlib_plugin.py:150: UserWarning: Float image out of standard range; displaying image with stretched contrast.
  lo, hi, cmap = _get_display_range(image)
Clipping input data to the valid range for imshow with RGB data ([0..1] for floats or [0..255] for integers).


```